

A terrestrial gamma-ray flash and ionospheric ultraviolet emissions powered by lightning

Torsten Neubert^{1*}, Nikolai Østgaard², Victor Reglero³, Olivier Chanrion¹, Matthias Heumesser¹, Krystallia Dimitriadou¹, Freddy Christiansen¹, Carl Budtz-Jørgensen¹, Irfan Kuvvetli¹, Ib Lundgaard Rasmussen¹, Andrey Mezentsev², Martino Marisaldi^{2,4}, Kjetil Ullaland², Georgi Genov², Shiming Yang², Pavlo Kochkin², Javier Navarro-Gonzalez³, Paul H. Connell³, Chris J. Eyles³

¹National Space Institute, Technical University of Denmark (DTU Space), Kongens Lyngby, Denmark. ²Birkeland Centre for Space Science, Department of Physics and Technology, University of Bergen, Bergen, Norway. ³Image Processing Laboratory, University of Valencia, Valencia, Spain. ⁴Astrophysics and Space Science Observatory, National Institute for Astrophysics, Bologna, Italy.

*Corresponding author. Email: neubert@space.dtu.dk

Terrestrial gamma-ray flashes (TGFs) are transient gamma-ray emissions from thunderstorms, generated by electrons accelerated to relativistic energies in electric fields. Elves are ultraviolet and optical emissions excited in the lower ionosphere by electromagnetic waves radiated from lightning current pulses. We observe a TGF and an associated Elve using the Atmosphere-Space Interactions Monitor on the International Space Station. The TGF occurs at the onset of a lightning current pulse that generates an Elve, in the early stage of a lightning flash. Our measurements suggest that the current onset is fast and has a high amplitude, a prerequisite for Elves, and that the TGF is generated in the electric fields associated with the lightning leader.

Transient luminous emissions (TLEs), such as Sprites, Jets and Elves, occur above thunderstorm clouds (1). Terrestrial gamma-ray flashes (TGFs) are brief (less than a few milliseconds) emissions of photons reaching energies of tens of MeV, observed by astrophysical satellites passing over thunderstorms (2–5). TGFs were initially thought to originate from high-altitude TLEs, where low atmospheric absorption would allow the TGF photons to escape, but their source was later determined to be within the thunderstorm clouds (6–8). It is now understood that TGFs are produced by bremsstrahlung radiation from electrons accelerated in thunderstorm electric fields, reaching energies in the runaway regime, where the cross sections for interactions decrease with further acceleration (9). To generate TGFs, seed electrons are needed in the runaway regime, e.g., released by cosmic ray interactions with the atmosphere (10), or from thermal electrons accelerated in the fields of lightning leader tips (11). The relativistic electron flux must then be amplified for the bremsstrahlung to reach the measured flux levels, as in relativistic runaway electron avalanches, possibly enhanced by feed-back effects from positrons created by pair-production and from ionization by backscattered bremsstrahlung (9). The role of the large-scale electric field in a cloud relative to the enhanced field at a lightning leader tip, however, is still debated (9–11).

We present observations with the Atmosphere-Space In-

teractions Monitor (ASIM), installed on the International Space Station (ISS), of a TGF produced in the initial stage of a lightning flash. The TGF was observed east of the island of Sulawesi in Indonesia on 2018 October 10, at 13:01:33.100080 Coordinated Universal Time (UTC). ASIM has two X- and gamma-ray detectors, three ultraviolet (UV) and optical photometers, and two optical imaging cameras (12–14). The instruments are pointed toward the nadir (directly downwards) to minimize gamma-ray flux losses due to atmospheric absorption. Figure 1, A and B, shows the location of the TGF, the surrounding cloud top altitudes derived from observations by the Himawari weather satellite (15), and the full and cropped field of view of the ASIM optical instruments. Figure 1C shows the projection of the ASIM camera image and the location of a coincident lightning event detected by the World Wide Lightning Location Network (WWLLN) (15).

The instrument data projections are to 12 km altitude, 1 km below the maximum altitude of the cloud top (Fig. 1C). The pointing direction of the sensors is determined from the ISS attitude and the nominal mounting of the ASIM platform. It is calibrated by assuming the WWLLN lightning location is at the maximum optical activity of the ASIM image. This correction is $\sim 1.4^\circ$, corresponding to 11.8 km at ground level, which also aligns the ASIM image of the cloud with its position in the Himawari data. The WWLLN light-

ning location has ~ 5 km uncertainty and occurred ~ 11 ms after the time estimated by the ASIM photometer pulses (15), which is within the ~ 20 ms uncertainty in the absolute timing signal received by ASIM from the ISS. The TGF source location is estimated from the angle of arrival of 70-350 keV photons to the ASIM low energy X-ray detector (LED). This angle is determined from the shadow pattern cast by a coded mask onto the pixelated detector plane. The relative pointing direction between the LED and the optical sensors has not been calibrated so we assume its nominal value (co-aligned). We conclude that the optical and X-ray measurements provide a consistent identification of this small (20 km^2) convective cloud as the source of the lightning associated with the TGF.

The signals of the three ASIM photometers around the time of the event are shown in Fig. 2. The photometers measure continuum emission in the UV band 180-235 nm, covering part of the Lyman-Birge-Hopfield (LBH) system of N_2 , and line emissions from N_2 2P at 337 nm (filter width 5 nm) and O I at 777.4 nm (filter width 3 nm), all at sample frequencies of 100,000 Hz. Also shown in Fig. 2 are the observations of the TGF, in photon counts measured by the low-energy X-ray detector (50-350 keV) and the high-energy detector (HED, 300 keV-30 MeV). The time resolution is $1 \mu\text{s}$ for the LED and 27 ns for the HED, and the relative timing accuracy between the optical sensors and LED/HED is $\pm 5 \mu\text{s}$.

The optical activity begins several milliseconds before the main optical pulses and intensifies at a time $t = -200 \mu\text{s}$, measured with respect to the onset of the HED pulse, signifying an increase of the lightning current. The onset of the TGF coincides with the onset of the UV emissions (to within $10 \mu\text{s}$) and an accelerated increase in the 337 nm and 777.4 nm signals appears as a change in their slope 0-60 μs after the TGF trigger (15). The TGF lasts about 30-40 μs and has a weaker tail extending to $\sim 80 \mu\text{s}$ for the high-energy photons (HED) and $\sim 200 \mu\text{s}$ for the low energy photons (LED), consistent with delays expected from Compton scattering of X- and gamma-rays in the atmosphere (16).

The emissions at 777.4 nm are from atomic oxygen and therefore from the current in a lightning leader channel, and the 337 nm emissions are mostly from the lightning discharge in the cloud (leader and streamers) (17) with negligible contributions from the ionosphere (i.e., an Elve) (18). UV emissions are strongly damped in the atmosphere, but are seen here with an amplitude that rises more rapidly than the optical signals, which is the signature of an Elve (18). Elves are quite common (19) ~ 1 ms duration emissions excited by the electromagnetic pulse (EMP) from the large current impulse of cloud-to-ground lightning (20) or intra-cloud lightning (21). The EMP energizes free electrons at the lower edge of the ionosphere at 80-90 km altitude, which

excite the atmospheric constituents. The radiation pattern from the lightning current onset excites rings of Elve emission centered above the lightning (for vertical lightning), which rapidly expand horizontally with detectable radii from ~ 50 to 400 km (22). The ASIM imaging cameras are not sufficiently sensitive to measure Elves because of their short duration and large spatial extent when observed toward the nadir, so we only analyze data from the photometers.

The UV Elve is detected with a delay corresponding to the travel times of the EMP to the ionosphere and of UV photons from the ionosphere to the instruments. The shortest combined path is approximately the direct path, considering the geometry of the observations (Fig. 3). We therefore consider the initiation of the UV pulse as coinciding with the initiation of the current pulse, which starts $\lesssim 10 \mu\text{s}$ after the onset of the TGF. The equivalent optical photons are scattered in the cloud, causing the optical pulse to broaden and the peak to be delayed by several hundred microseconds or more, depending on the optical depth of the source and on the cloud properties (23). This is consistent with the UV and optical pulses we observe (Fig. 2B). The characteristics of the optical pulses also resemble those of lightning emissions observed by the Fast On-orbit Rapid Recording of Transient Events (FORTE) satellite (24). This suggests that the current source lifetime is much shorter than the optical pulses, although we cannot characterize the pulse current further from optical measurements alone. The first optical photons to arrive at the sensors are those that have undergone the least scattering in the cloud. A pulse is first detected by ASIM when the flux-levels are above the sensor sensitivity thresholds and the onset of a pulse may therefore appear with a delay. For this event, the optical pulses are bright and rising out of pre-activity, suggesting that a delay from the limits of the sensor sensitivities and of cloud scattering are minor and that the optical pulses, therefore, should start at approximately the same time as the UV pulse, as observed.

The photometer measurements are shown on a logarithmic scale in Fig. 4. The TGF and the associated high-amplitude pulses occur ~ 5 ms after the beginning of the lightning flash (Fig. 4B), consistent with studies of radio emissions from TGF-producing flashes (25). The flash fades over ~ 280 ms, terminating with two smaller optical pulses (Fig. 4A). The onset of the emission at $t = -5$ ms could reflect the time when an upward propagating lightning leader first becomes detectable in the cloud, or it may reflect the onset of the formation of the leader. The start of the leader emission is modulated by 2 larger oscillations (Fig. 4B), possibly related to the leader propagation, and the continuation after the TGF could reflect the continued propagation of the leader upwards/horizontally into a positive charge layer, as

has been previously proposed (26). However, cloud scattering is too strong to identify the spatial propagation of the leader from the camera images.

Although TGF-type emissions have been observed from leaders propagating to the ground (27), we reject that scenario as an explanation of this event, because of the strong photon absorption that would occur in the lower atmosphere (9). Instead, we interpret this event as an intra-cloud lightning flash of positive polarity (Fig. 3) where the electric field ahead of the leader plays a role in producing the TGF.

The Elve requires a high-amplitude lightning current pulse with a fast rise time, which suggests the formation of, or access to, a large charge reservoir within the cloud that is rapidly drained. The reservoir could be formed by the ionizing avalanche of the relativistic electrons or by the formation of an extended streamer corona, as suggested by radio signal studies of TGFs (28–30). It is likely that further current amplification is required to produce an Elve. Pulses with high currents have been identified in radio observations and have been associated with TGFs (31). They are termed positive energetic in-cloud pulses (+EIPs); they last ~50 μ s and may reach hundreds of kA (31). +EIPs occur typically in the upper regions of clouds after a few milliseconds of ascending negative leader activity, and it has been suggested that they can generate TGFs and Elves simultaneously (31). The TGF in this event is relatively short in duration compared to past observations (2–5). A short duration was predicted for TGFs accompanied by Elves, because Elves require lightning source currents that vary more rapidly (31). The optical pulses we observe may then be the counterpart of radio +EIPs.

Our observations illustrate the temporal sequence of emissions in optical, UV, X-ray and gamma-rays bands with a time resolution of 10 μ s and simultaneous imaging of a TGF in hard X-rays and optical images. The observations provide evidence that there is a connection between TLEs and TGFs after all.

REFERENCES AND NOTES

1. V. P. Pasko, Y. Yair, C. L. Kuo, Lightning related transient luminous events at high altitude in the Earth's atmosphere: Phenomenology, mechanisms and effects. *Space Sci. Rev.* **168**, 475–516 (2012). doi:10.1007/s11214-011-9813-9
2. G. J. Fishman, P. N. Bhat, R. Mallozzi, J. M. Horack, T. Koshut, C. Kouveliotou, G. N. Pendleton, C. A. Meegan, R. B. Wilson, W. S. Paciesas, S. J. Goodman, H. J. Christian, Discovery of intense gamma-ray flashes of atmospheric origin. *Science* **264**, 1313–1316 (1994). doi:10.1126/science.264.5163.1313 Medline
3. D. M. Smith, L. I. Lopez, R. P. Lin, C. P. Barrington-Leigh, Terrestrial gamma-ray flashes observed up to 20 MeV. *Science* **307**, 1085–1088 (2005). doi:10.1126/science.1107466 Medline
4. M. Marisaldi, F. Fuschino, C. Labanti, M. Galli, F. Longo, E. Del Monte, G. Barbiellini, M. Tavani, A. Giuliani, E. Moretti, S. Vercellone, E. Costa, S. Cutini, I. Donnarumma, Y. Evangelista, M. Feroci, I. Lapshov, F. Lazzarotto, P. Lipari, S. Mereghetti, L. Pacciani, M. Rapisarda, P. Soffitta, M. Trifoglio, A. Argan, F. Boffelli, A. Bulgarelli, P. Caraveo, P. W. Cattaneo, A. Chen, V. Cocco, F. D'Ammando, G. De Paris, G. Di Cocco, G. Di Persio, A. Ferrari, M. Fiorini, T. Froyland, F. Gianotti, A. Morselli, A. Pellizzoni, F. Perotti, P. Picozza, G. Piano, M. Pilia, M. Prest, G. Pucella, A. Rappoldi, A. Rubini, S. Sabatini, E. Striani, A. Trois, E. Vallazza, V. Vittorini, A. Zambra, D. Zanello, L. A. Antonelli, S. Colafrancesco, D. Gasparri, P. Giommi, C. Pittori, B. Preger, P. Santolamazza, F. Verrecchia, L. Salotti, Detection of terrestrial gamma ray flashes up to 40 MeV by the AGILE satellite. *J. Geophys. Res.* **115**, A00E13 (2010). doi:10.1029/2009JA014502
5. O. J. Roberts, G. Fitzpatrick, M. Stanbro, S. McBreen, M. S. Briggs, R. H. Holzworth, J. E. Grove, A. Chekhtman, E. S. Cramer, B. G. Mailyan, The first Fermi-GBM terrestrial gamma ray flash catalog. *J. Geophys. Res. Space Phys.* **123**, 4381–4401 (2018). doi:10.1029/2017JA024837
6. S. A. Cummer *et al.*, Measurements and implications of the relationship between lightning and terrestrial gamma ray flashes. *Geophys. Res. Lett.* **32**, L08811 (2005). doi:10.1029/2005GL022778
7. M. A. Stanley, X.-M. Shao, D. M. Smith, L. I. Lopez, M. B. Pongratz, J. D. Harlin, M. Stock, A. Regan, A link between terrestrial gamma-ray flashes and intracloud lightning discharges. *Geophys. Res. Lett.* **33**, L06803 (2006). doi:10.1029/2005GL025537
8. J. R. Dwyer, D. M. Smith, A comparison between Monte Carlo simulations of runaway breakdown and terrestrial gamma-ray flash observations. *Geophys. Res. Lett.* **32**, L22804 (2005). doi:10.1029/2005GL023848
9. J. R. Dwyer, D. M. Smith, S. A. Cummer, High-energy atmospheric physics: Terrestrial gamma-ray flashes and related phenomena. *Space Sci. Rev.* **173**, 133–196 (2012). doi:10.1007/s11214-012-9894-0
10. A. V. Gurevich, G. M. Milikh, R. A. Roussel-Dupré, Runaway electron mechanism of air breakdown and preconditioning during a thunderstorm. *Phys. Lett. A* **165**, 463–468 (1992). doi:10.1016/0375-9601(92)90348-P
11. L. P. Babich, E. I. Bochkov, I. M. Kutsyk, T. Neubert, O. Chanrion, Analyses of electron runaway in front of the negative streamer channel. *J. Geophys. Res.* **122**, 8974–8984 (2017). doi:10.1002/2017JA023917
12. T. Neubert, N. Østgaard, V. Reglero, E. Blanc, O. Chanrion, C. A. Oxborrow, A. Orr, M. Tacconi, O. Hartnack, D. D. V. Bhandari, The ASIM mission on the International Space Station. *Space Sci. Rev.* **215**, 26 (2019). doi:10.1007/s11214-019-0592-z
13. N. Østgaard, J. E. Balling, T. Bjørnsen, P. Brauer, C. Budtz-Jørgensen, W. Buijwan, B. Carlson, F. Christiansen, P. Connell, C. Eyles, D. Fehlker, G. Genova, P. Grudziński, P. Kochkin, A. Kohfeldt, I. Kuvvetli, P. L. Thomsen, S. M. Pedersen, J. Navarro-Gonzalez, T. Neubert, K. Njøten, P. Orleanski, B. H. Qureshi, L. R. Cenkeramaddi, V. Reglero, M. Reina, J. M. Rodrigo, M. Rostad, M. D. Sabau, S. S. Kristensen, Y. Skogseide, A. Solberg, J. Stadsnes, K. Ullaland, S. Yang, The Modular X- and 1 Gamma-ray Sensor (MXGS) of the ASIM payload on the International Space Station. *Space Sci. Rev.* **215**, 23 (2019). doi:10.1007/s11214-018-0573-7
14. O. Chanrion, T. Neubert, I. Lundgaard Rasmussen, C. Stoltze, D. Tcherniak, N. C. Jessen, J. Polny, P. Brauer, J. E. Balling, S. Savstrup Kristensen, S. Forchhammer, P. Hofmeyer, P. Davidsen, O. Mikkelsen, D. Bo Hansen, D. D. V. Bhandari, C. G. Petersen, M. Lorenzen, The Modular Multispectral Imaging Array (MMIA) of the ASIM payload on the International Space Station. *Space Sci. Rev.* **215**, 28 (2019). doi:10.1007/s11214-019-0593-y
15. See supplementary materials.
16. S. Celestin, V. P. Pasko, Compton scattering effects on the duration of terrestrial gamma-ray flashes. *Geophys. Res. Lett.* **39**, L02802 (2012). doi:10.1029/2011GL0150342
17. R. A. Armstrong, J. A. Shorter, M. J. Taylor, D. M. Suszcynsky, W. A. Lyons, L. S. Jeong, Photometric measurements in the SPRITES '95 & '96 campaigns of nitrogen second positive (399.8 nm) and first negative (427.8 nm) emissions. *J. Atmos. Sol. Terr. Phys.* **60**, 787–799 (1998). doi:10.1016/S1364-6826(98)00026-1
18. F. J. Pérez-Invernón, A. Luque, F. J. Gordillo-Vázquez, Modeling the chemical impact and the optical emissions produced by lightning-induced electromagnetic fields in the upper atmosphere: The case of halos and elves

- triggered by different lightning discharges. *J. Geophys. Res.* **123**, 7615–7641 (2018).
19. A. B. Chen, C.-L. Kuo, Y.-J. Lee, H.-T. Su, R.-R. Hsu, J.-L. Chern, H. U. Frey, S. B. Mende, Y. Takahashi, H. Fukunishi, Y.-S. Chang, T.-Y. Liu, L.-C. Lee, Global distributions and occurrence rates of transient luminous events. *J. Geophys. Res.* **113**, A08306 (2008). [doi:10.1029/2008JA013101](https://doi.org/10.1029/2008JA013101)
 20. U. S. Inan, W. A. Sampson, Y. N. Taranenko, Space-time structure of optical flashes and ionization changes produced by lightning-emp. *Geophys. Res. Lett.* **23**, 133–136 (1996). [doi:10.1029/95GL03816](https://doi.org/10.1029/95GL03816)
 21. R. A. Marshall, C. L. da Silva, V. P. Pasko, Elve doublets and compact intracloud discharges. *Geophys. Res. Lett.* **42**, 6112–6119 (2015). [doi:10.1002/2015GL064862](https://doi.org/10.1002/2015GL064862)
 22. C. L. Kuo, T.-Y. Huang, S. C. Chang, J. K. Chou, L. J. Lee, Y. J. Wu, A. B. Chen, H. T. Su, R. R. Hsu, H. U. Frey, S. B. Mende, Y. Takahashi, L. C. Lee, Full-kinetic elve model simulations and their comparisons with the ISUAL observed events. *J. Geophys. Res.* **117**, A07320 (2012). [doi:10.1029/2012JA017599](https://doi.org/10.1029/2012JA017599)
 23. T. E. Light, D. M. Suszcynsky, M. W. Kirkland, A. R. Jacobson, Simulations of lightning optical waveforms as seen through clouds by satellites. *J. Geophys. Res.* **106**, 17103–17114 (2001). [doi:10.1029/2001JD900051](https://doi.org/10.1029/2001JD900051)
 24. T. E. Light, D. M. Suszcynsky, A. R. Jacobson, Coincident radio frequency and optical emissions from lightning, observed with the FORTE satellite. *J. Geophys. Res.* **106**, 28223–28231 (2001). [doi:10.1029/2001JD000727](https://doi.org/10.1029/2001JD000727)
 25. S. A. Cummer, F. Lyu, M. S. Briggs, G. Fitzpatrick, O. J. Roberts, J. R. Dwyer, Lightning leader altitude progression in terrestrial gamma-ray flashes. *Geophys. Res. Lett.* **42**, 7792–7798 (2015). [doi:10.1002/2015GL065228](https://doi.org/10.1002/2015GL065228)
 26. R. U. Abbasi *et al.*, Gamma ray showers observed at ground level in coincidence with downward lightning leaders. *J. Geophys. Res.* **123**, 6864–6879 (2018).
 27. X.-M. Shao, T. Hamlin, D. M. Smith, A closer examination of terrestrial gamma-ray flash-related lightning processes. *J. Geophys. Res.* **115**, A00E30 (2010). [doi:10.1029/2009JA014835](https://doi.org/10.1029/2009JA014835)
 28. B. G. Mailyan, A. Nag, M. J. Murphy, M. S. Briggs, J. R. Dwyer, W. Rison, P. R. Krehbiel, L. Boggs, A. Bozarth, E. S. Cramer, O. J. Roberts, M. Stanbro, H. K. Rassoul, Characteristics of radio emissions associated with terrestrial gamma-ray flashes. *J. Geophys. Res.* **123**, 5933–5948 (2018). [doi:10.1029/2018JA025450](https://doi.org/10.1029/2018JA025450)
 29. F. Lyu, S. A. Cummer, P. R. Krehbiel, W. Rison, M. S. Briggs, E. Cramer, O. Roberts, M. Stanbro, Very high frequency radio emissions associated with the production of terrestrial gamma-ray flashes. *Geophys. Res. Lett.* **45**, 2097–2105 (2018). [doi:10.1002/2018GL077102](https://doi.org/10.1002/2018GL077102)
 30. F. Lyu, S. A. Cummer, M. Briggs, M. Marisaldi, R. J. Blakeslee, E. Bruning, J. G. Wilson, W. Rison, P. Krehbiel, G. Lu, E. Cramer, G. Fitzpatrick, B. Mailyan, S. McBreen, O. J. Roberts, M. Stanbro, Ground detection of terrestrial gamma ray flashes from distant radio signals. *Geophys. Res. Lett.* **43**, 8728–8734 (2016). [doi:10.1002/2016GL070154](https://doi.org/10.1002/2016GL070154)
 31. N. Y. Liu, J. R. Dwyer, S. A. Cummer, Elves accompanying terrestrial gamma ray flashes. *J. Geophys. Res. Space Phys.* **122**, 10563–10576 (2017). [doi:10.1002/2017JA024344](https://doi.org/10.1002/2017JA024344)
 32. Japan Aerospace Exploration Agency (JAXA), www.eorc.jaxa.jp/ptree/index.html.
 33. K. Bessho, K. Date, M. Hayashi, A. Ikeda, T. Imai, H. Inoue, Y. Kumagai, T. Miyakawa, H. Murata, T. Ohno, A. Okuyama, R. Oyama, Y. Sasaki, Y. Shimazu, K. Shimoji, Y. Sumida, M. Suzuki, H. Taniguchi, H. Tsuchiyama, D. Uesawa, H. Yokota, R. Yoshida, An Introduction to Himawari-8/9, Japan's new-generation geostationary meteorological satellites. *J. Meteorol. Soc. Jpn.* **94**, 151–177 (2016). [doi:10.2151/jmsj.2016-009](https://doi.org/10.2151/jmsj.2016-009)
 34. University of Wyoming, <http://weather.uwyo.edu/upperair/sounding.html>.
 35. M. L. Hutchins, R. H. Holzworth, J. B. Brundell, C. J. Rodger, Relative detection efficiency of the World Wide Lightning Location Network. *Radio Sci.* **47**, RS6005 (2012). [doi:10.1029/2012RS005049](https://doi.org/10.1029/2012RS005049)

ACKNOWLEDGMENTS

We thank Maribeth Stolzenburg and Michael Rycroft for valuable comments, and the World Wide Lightning Location Network for the lightning location data used in this paper; **Funding:** ASIM is a mission of the European Space Agency (ESA), funded by ESA and national grants of Denmark, Norway and Spain. ESA PRODEX contracts C 4000115884 (DTU) and 4000123438 support the ASIM Science Data Centre (Bergen). The science analysis is supported by: ESA Topical Team contract 4200019920/06/NL/VJ; the European Commission, Innovative Training Network SAINT, project grant 722337-SAINT; the European Research Council grant AdG - FP7/2007-2013: n 320839; the Research Council of Norway contracts 223252/F50 and 208028/F50 (CoE/BCSS); and The Ministerio Ciencia, Innovacion y Universidades grant ESP 2017- 86263-C4. **Author contributions:** T.N. leads the ASIM project. N.Ø. leads the LED and HED instrument consortia, supported by C.B.-J. and I.K. V.R. leads the LED imaging analysis, supported by J.N.-G. and P.H.C. O.C. leads the optical instrument consortium supported by M.H. and K.D. F.C. performed in-orbit LED health analysis and I.L.R. in-flight calibration of the photometers. K.U., G.G., S.Y., P.K., C.J.E. conducted LED and HED in-orbit commissioning and M.M., A.M. performed LED and HED data analysis. **Competing interests:** The authors declare no competing interests. **Data and materials availability:** The ASIM data for this event are provided in Data S1-S5. The WWLLN lightning data, cloud data and ISS attitude data are provided in the Supplementary Materials.

SUPPLEMENTARY MATERIALS

science.sciencemag.org/cgi/content/full/science.aax3872/DC1

Materials and Methods

Supplementary Text

Fig. S1

Data S1 to S5

References (32–35)

2 April 2019; accepted 31 October 2019

Published online 10 December 2019

10.1126/science.aax3872

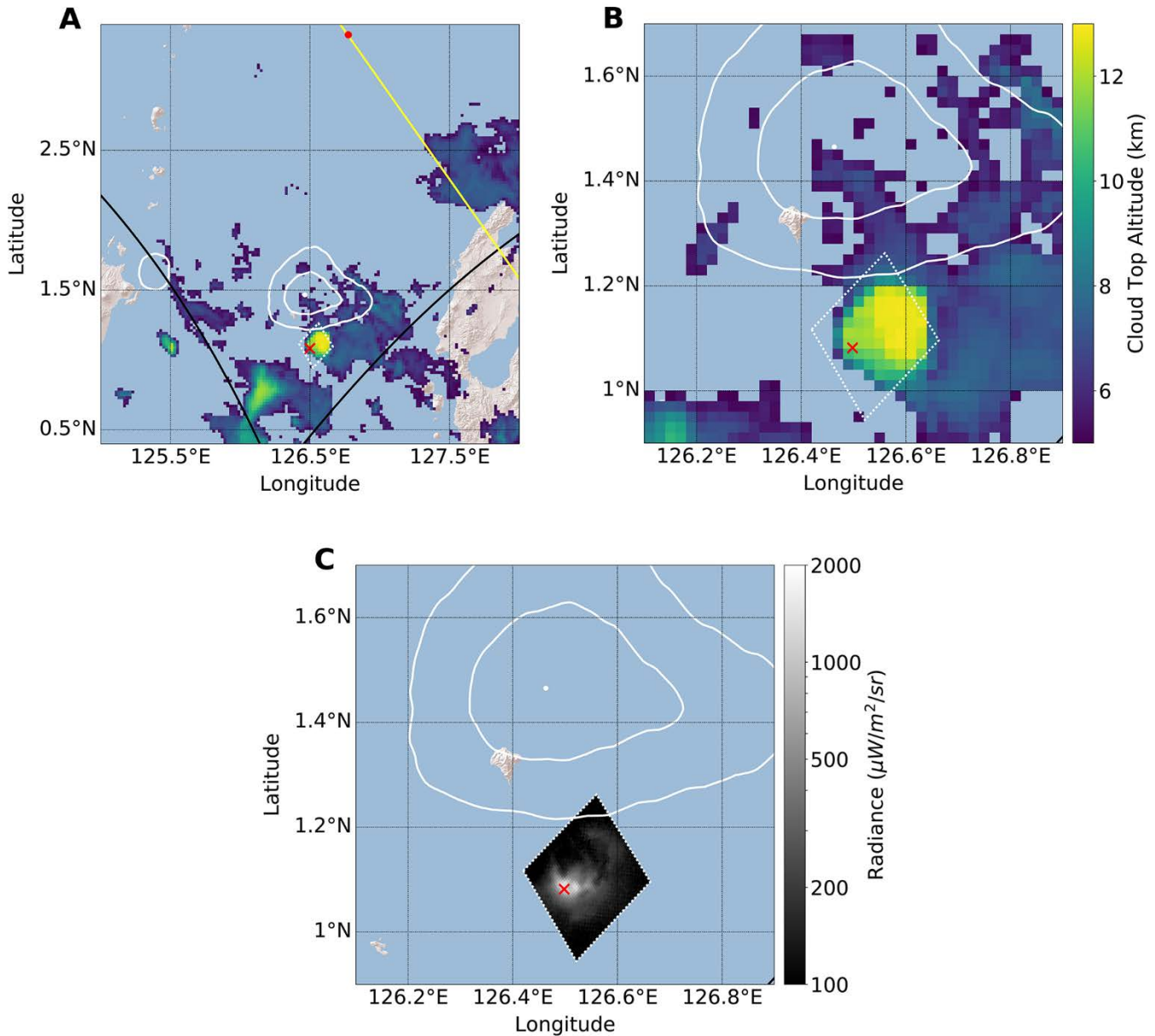


Fig. 1. Location of the TGF event observed on 2018 October 10. (A) Cloud top altitudes (15) are shown in color. The ISS orbit is shown by the yellow curve and the red dot marks its position at the onset time of the TGF at 13:01:33.100080 UTC. The white dot marks the most probable TGF location, with white contours outlining the 68% and 95.4% confidence regions. The black box is the full field of view of the optical instruments, and the white dash-lined box the cropped images downlinked from the ISS. (B) The same view zoomed in to the active cloud region. A single thundercloud partially overlaps with the TGF 95% confidence region. (C) The TGF position overlain with a projection of the ASIM camera image in the 337 nm filter, with 83 ms exposure. A coincident lightning event detected by the WWLLN (15) is shown with a red cross. The attitude of the ASIM instruments is calibrated to align the WWLLN lightning location with the maximum optical activity of the ASIM image.

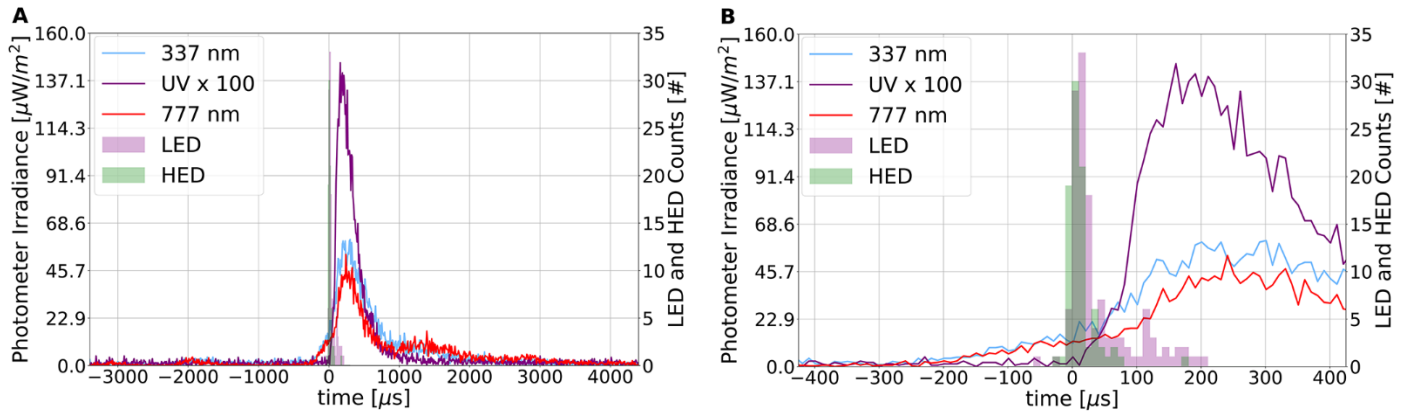


Fig. 2. Light curves of the event. The gamma-flash trigger time is at $t = 0$ which corresponds to 13:01:33.100080 UTC. (A) Photometer (left axis), X-ray and gamma-ray (right axis) measurements around the time of the event. LED is the low-energy X-ray detector (50-350 keV) and HED the high-energy detector (300 keV-30 MeV). The UV photometer measures 180-235 nm and is multiplied by 100 to show on the same scale as the optical photometers. All three photometers sample at 100 kHz. (B) The same data shown zoomed in further at the time of the TGF.

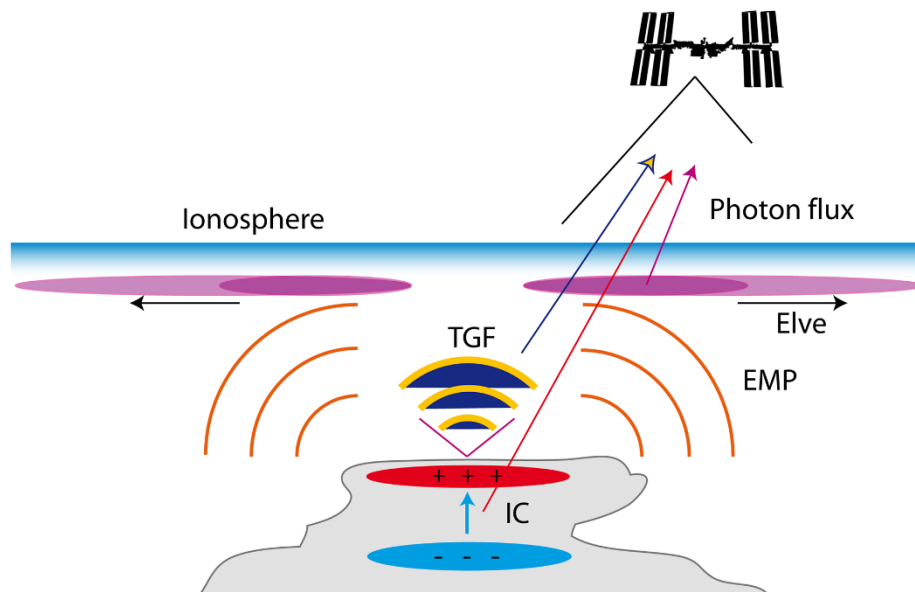


Fig. 3. Our proposed scenario. An intra-cloud (IC) lightning event generates a TGF and electromagnetic pulse (EMP). The EMP excites expanding waves of UV emission in the lower ionosphere (Elve). TGF and UV emissions are observed by ASIM on the ISS (arrows). The grey bar at the bottom is the ground.

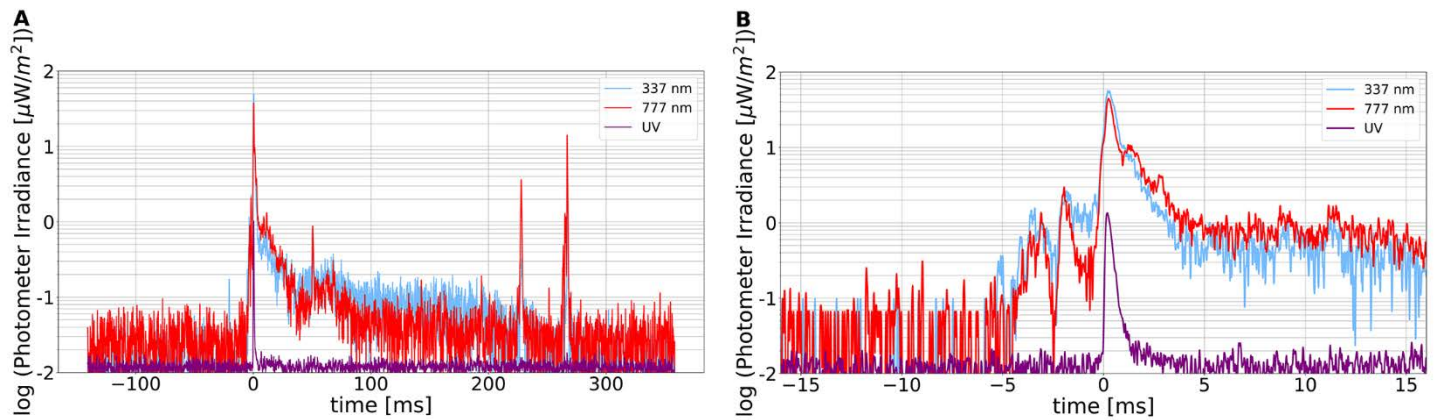


Fig. 4. Analysis of the lightning flash. (A) The same data as Fig. 2 but on a logarithmic scale and smoothed by a Gaussian filter with width $\sigma = 10$ samples. Two additional optical pulses occur 200-300 ms after the initial flash. (B) The same data zoomed in to the start of the flash smoothed with $\sigma = 2$ samples. Optical emission begins 5 ms prior to UV emission and the TGF.

A terrestrial gamma-ray flash and ionospheric ultraviolet emissions powered by lightning

Torsten Neubert, Nikolai Østgaard, Victor Reglero, Olivier Chanrion, Matthias Heumesser, Krystallia Dimitriadou, Freddy Christiansen, Carl Budtz-Jørgensen, Irfan Kuvvetli, Ib Lundgaard Rasmussen, Andrey Mezentsev, Martino Marisaldi, Kjetil Ullaland, Georgi Genov, Shiming Yang, Pavlo Kochkin, Javier Navarro-Gonzalez, Paul H. Connell and Chris J. Eyles

published online December 11, 2019

ARTICLE TOOLS

<http://science.sciencemag.org/content/early/2019/12/09/science.aax3872>

SUPPLEMENTARY MATERIALS

<http://science.sciencemag.org/content/suppl/2019/12/09/science.aax3872.DC1>

REFERENCES

This article cites 35 articles, 2 of which you can access for free
<http://science.sciencemag.org/content/early/2019/12/09/science.aax3872#BIBL>

PERMISSIONS

<http://www.sciencemag.org/help/reprints-and-permissions>

Use of this article is subject to the [Terms of Service](#)

Science (print ISSN 0036-8075; online ISSN 1095-9203) is published by the American Association for the Advancement of Science, 1200 New York Avenue NW, Washington, DC 20005. The title *Science* is a registered trademark of AAAS.

Copyright © 2019, American Association for the Advancement of Science